Eur. Phys. J. A **1**, 261–266 (1998)

THE EUROPEAN PHYSICAL JOURNAL A

γ Spectroscopy of ^{209}Pb with deep inelastic reactions

M. Rejmund[1,2], K.H. Maier[3], R. Broda[4], B. Fornal[4], M. Lach[4], J. Wrzesiński[4], J. Blomqvist[5], A. Gadea[6], J. Gerl[1], M. Górska[1,2], H. Grawe[1], M. Kaspar[1], H. Schaffner[1], Ch. Schlegel[1], R. Schubart[1], H.J. Wollersheim[1]

[1] Gesellschaft für Schwerionenforschung, Planck Strasse 1, D-64291 Darmstadt, Germany
[2] Nuclear Physics Division, Institute of Experimental Physics, Warsaw University, Poland
[3] Hahn-Meitner-Institut, Berlin, Germany
[4] Niewodniczański Institute of Nuclear Physics, Cracow, Poland
[5] Royal Institute of Technology, Physics Department Frescati, Stockholm, Sweden
[6] Instituto Nazionale di Fisica Nucleare, Laboratori Nazionali di Legnaro, Legnaro, Italy

Received: 22 November 1997
Communicated by D. Schwalm

Abstract. High spin states in nuclei around ^{208}Pb were populated in deep inelastic collisions of ^{76}Ge, ^{136}Xe, and ^{208}Pb projectiles with ^{208}Pb targets at beam energies about 12% above the Coulomb barrier. New states in ^{209}Pb were found by measuring γ-γ-coincidences. They are interpreted as the yrast states that originate from the coupling of one neutron to the lowest excitations of the ^{208}Pb core. The results are discussed in the frame of the shell model.

PACS. 21.60.Cs Shell model – 23.20.Lv Gamma transitions and level energies – 27.80.+w $190 \le A \le 219$ – 25.70.-z Low and intermediate energy heavy-ion reactions

1 Introduction

^{209}Pb consists of the doubly magic ^{208}Pb plus one neutron and has therefore been of high interest since the introduction of the shell model. It has been studied by the (d,p) reaction (neutron stripping) on the stable ^{208}Pb target nucleus [1], the (p,d) reaction (neutron pick up) on the radioactive ^{210}Pb target [2], the (t,α) reaction (proton pick up) on ^{210m}Bi with a radioactive beam and target [3], and the two neutron stripping reaction ^{207}Pb(t,p)^{209}Pb [4]. γ transitions in ^{209}Pb have only been measured with the ^{208}Pb(d,p γ)^{209}Pb reaction [5] and following the β decay of ^{209}Tl [6]. All of the above mentioned reactions populate single particle states or selected two particle one hole states. In this paper we present the results of yrast γ ray spectroscopy of ^{209}Pb performed using deep inelastic heavy ion reactions with different projectiles on a ^{208}Pb target. This reaction mechanism populates high spin states in stable and moderately neutron rich nuclei that cannot be reached with fusion-evaporation reactions [7,8]. The levels close to the yrast line are often of simple structure; therefore their measured properties can be interpreted to yield rather directly the shell-model interaction. The experiments, as presented in the next section, gave information on new γ transitions from high spin states in ^{210}Pb [9] and several other nuclei around ^{208}Pb. Here we limit ourselves to results on ^{209}Pb.

Attempts to derive the shell model interaction from the interaction between free nucleons have been made already [10] years ago and have been quite successful [11]. There is renewed interest in this field, as the advances of computers have removed previous computational limitations. Much of the corresponding experimental information is still missing. The present study is part of an effort to fill some of these gaps.

2 Experiments

Two experiments have been performed at the UNILAC accelerator of GSI to study nuclei around ^{208}Pb. A 30 mg/cm^2 ^{208}Pb target (98.7% enriched) was hit by a beam of 6.5 A·MeV ^{208}Pb and 5.7 A·MeV ^{136}Xe ions. These beam energies were selected to give about 12% excess energy over the Coulomb barrier, because such conditions had been used successfully with lighter ion beams [8]. At the full beam energy deep inelastic reactions prevail, resulting in transfer of many particles, high angular momentum and large excitation energy. When the beam is slowed down towards the Coulomb barrier in the thick target, the reaction mechanism changes gradually to quasi elastic reactions. The data of a third experiment [12] at the ALPI accelerator of INFN Legnaro with the GASP γ spectrometer have also been used. This experiment used a 420 MeV ^{76}Ge beam on a thick ^{208}Pb target to study primarily neutron rich nuclei in the Ni to Ge region.

About 200 different nuclei have been produced and identified in one reaction of this type [13]. The predomi-

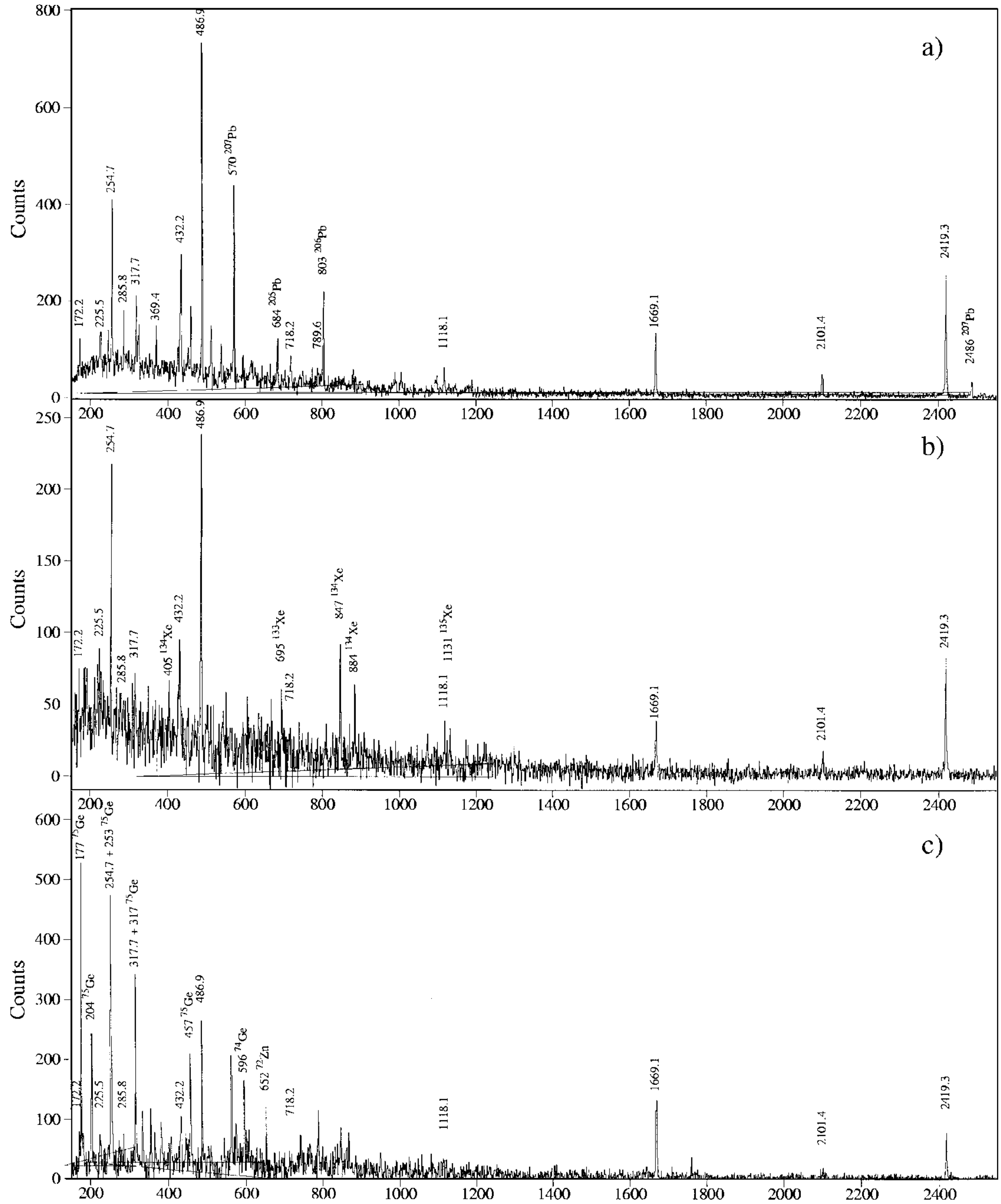

Fig. 1. Spectrum of prompt γ-rays in coincidence with the 1422.7 keV line from the experiments with **a** ^{208}Pb beam, **b** ^{136}Xe beam and **c** ^{76}Ge beam

nant part of γ rays is emitted from stopped nuclei and γ-γ-coincidences of the resulting sharp lines can resolve the spectra from different nuclei. The γ rays, emitted before the nucleus is stopped, (~ 3 ps) are Doppler broadened and contribute to the unresolved background. An important feature of deep inelastic reactions is a strong trend to equilibrate the N/Z ratio of the two colliding nuclei. Therefore neutron rich projectiles have been chosen, to favour production of the neutron rich nuclei of interest. The release of thermal energy by the evaporation of secondary neutrons from the excited reaction products limits the access to the very neutron rich region. Many experiments of this type have now shown, that transitions between yrast states dominate the measured spectra. This enables to study high spin states in nuclei, that cannot be reached in fusion-evaporation reactions, as is also the case for the presently studied ^{209}Pb.

The experiments at GSI used the set up [14] consisting of five EUROBALL Ge-cluster detectors [15] and 132 NaI detectors of the CRYSTAL BALL [16]. The Ge-detectors, placed at $\sim 154^0$ angle to the beam direction, had a total photo-peak efficiency of $\sim$2.2% at 1.33 MeV and the CRYSTAL BALL $\sim 53\%$. The width of the macro pulses of the beam was ≤ 5 ms with a repetition time of 20 ms. The

Table 1. Energies and intensities of γ-transitions in ^{209}Pb. Relative intensities in prompt coincidence with the 1422.7 keV transition from the experiment with the ^{208}Pb beam are presented. The last 3 transitions marked by †are from coincidences with the 2419.3 keV line. Energy and spin of the decaying levels are also given
‡- Multiple line, intensity uncertain

E_γ [keV]	I_γ	E_i [keV]	I_i^π
172.2 (3)	12 (2)	4756	
225.5 (2)	10 (2)	6099	
254.7 (1)	33 (3)	4584	
285.8 (3)	9 (2)	3810	$(21/2^-)$
317.7 (2)	18 (2)	3842	$(21/2^+)$
369.4 (2)	9 (2)	4698	
432.2 (3)	31 (10) ‡	3524	$(19/2^-)$
486.9 (1)	83 (5)	4329	$(23/2^+)$
718.2 (3)	10 (1)	3810	$(21/2^-)$
789.6 (4)	5 (1)	6432	
1118.1 (2)	11 (2)	5874	
1624 (1)	≤ 5	3047	$(15/2)^-$
1669.1 (2)	33 (3)	3092	$(17/2^-)$
2101.4 (3)	17 (2)	3524	$(19/2^-)$
2419.3 (1)	100 (7)	3842	$(21/2^+)$
643.5 (2)	13 (2) †	1423	$15/2^-$
779.2 (2)	14 (2) †	779	$11/2^+$
1422.7 (1)	100 (7) †	1423	$15/2^-$

data recorded during the macro pulse were distinguished from those outside it, separating prompt and short lived radiation from long lived decays. The microstructure of the beam consisted of ~1 ns wide pulses with a separation of 110 ns. Energies and times of all Ge- and NaI-detectors were measured. A coincidence between two Ge-detectors constituted a valid event. The beam pulse that caused the reaction was identified by detecting at least multiplicity 3 in the CRYSTAL BALL. No isomers have been found in ^{209}Pb. The analysis was therefore based on prompt spectra, as shown in Fig 1, with the requirement that both coincident pulses occurred between 30 ns before and 90 ns after the same beam pulse. A very high yield of Pb X-rays in the experiment with the ^{208}Pb beam made it necessary to use absorbers of 0.5 mm Ta and 0.5 mm Cu in front of the Ge-detectors. Consequently the efficiency at γ energies below 200 keV was significantly reduced. The γ efficiency has been measured with standard sources at the target position. The spectrum of Fig. 1c, measured with the GASP array shows best the low energy part of the spectrum, where several strong lines from the complementary reaction partner ^{75}Ge are seen. The high energy lines are more prominent in the data taken at GSI.

3 Results

New γ transitions in ^{209}Pb were identified from the spectra in prompt coincidence with the previously known γ rays of energy 1422.7 keV, 779.2 keV and 643.5 keV [1]. Figure 1 shows the γ-ray energy spectra coincident with the 1422.7 keV line in ^{209}Pb from the experiments with ^{208}Pb, ^{136}Xe and ^{76}Ge beams (panels a, b and c respectively). Transitions from the partner nucleus of the binary reaction, namely ^{207}Pb, ^{135}Xe, and ^{75}Ge respectively, are also evident. Also lines in the nuclei ^{206}Pb, ^{134}Xe and ^{74}Ge, which result from the reaction partner with the evaporation of one neutron, are clearly present in the corresponding spectra. The comparison of the spectra measured with different beams identifies these lines clearly and prevents otherwise possible misassignment to ^{209}Pb. Table 1 lists energies and relative intensities of γ transitions assigned to ^{209}Pb from the measurement with the ^{208}Pb beam. The yrast level scheme of excited states in ^{209}Pb presented in Fig. 2a was deduced from mutual prompt coincidence relations and relative intensities of γ transitions.

Although in deep inelastic reactions almost exclusively yrast states are populated, it was possible to observe a weak population of non yrast states via the quasielastic process. We observed the previously known [1] cascade of γ rays of energies 1567 keV, 465 keV and 285 keV feeding the ground state of ^{209}Pb; the levels at 1567 and 2032 keV energy are the single neutron $3d_{5/2}$ and $4s_{1/2}$ states, populated strongly in neutron transfer. The 285 keV line deexcites a $3/2^-$ level at 2317 keV [5] that is mainly $\nu 2g_{9/2} \otimes 3^-$. These low spin states are not shown in Fig. 2a.

Several other weak transitions were identified with ^{209}Pb. However, their definite placement in the level scheme could not be established from the present data. An 1100 keV transition is certainly located above the 3842 keV level likely feeding the 4329 keV state. A weak 1178 keV transition and a cascade of 790 keV and 458 keV γ rays were observed on top of the 3842 keV level. Also 1910 keV and 2020 keV transitions were found that feed the 1423 keV excited state.

The present experiments gave neither angular distributions of the γ-transitions nor any other direct information on level spins and transition multipolarities. The tentative spin assignments in Fig. 2 therefore rest upon the combination of the information from this experiment and others and upon theoretical expectations, that are reliable for the lower lying yrast states.

4 Interpretation

The measured level scheme of ^{209}Pb is shown in Fig. 2a and discussed with the help of columns b - d of Fig. 2. Column d shows the single particle and two particle-one hole configurations that are relevant for the discussion of yrast states at their unperturbed energies. A shell model calculation of the two particle-one hole states has been performed with empirical residual interactions from neighbouring nuclei, but without configuration mixing. The ma-

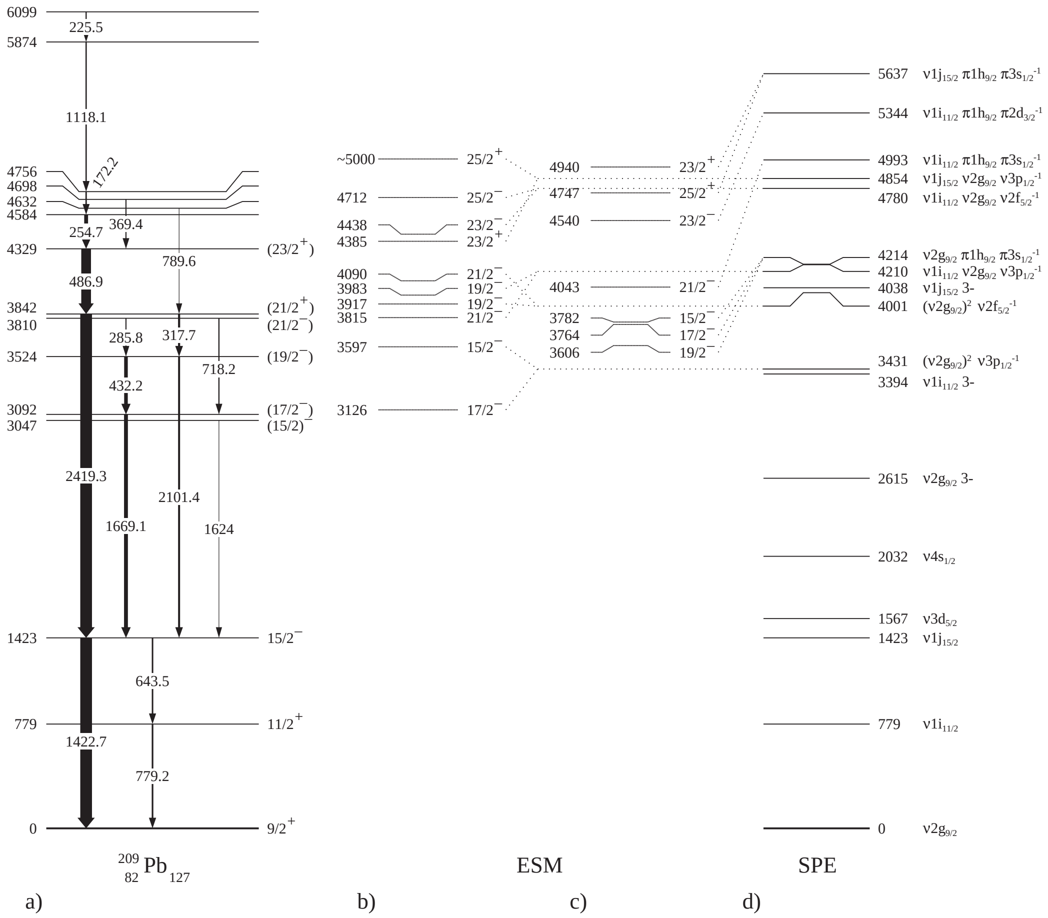

Fig. 2. Comparison of the experimental **a** level scheme of ^{209}Pb with shell-model expectations. Column **d** shows the unperturbed energies of the relevant configurations. Columns **b** and **c** give the energies calculated for the states of highest spins with residual interactions but without configuration mixing; **b** neutron and **c** proton excitations of ^{208}Pb core. See also text in particular for spin assignments

trix elements are given by:

$$\begin{aligned}
&\left\langle (j_1 j_2)_{J_c'}, j_3; J|H|(j_1 j_2)_{J_c}, j_3; J \right\rangle \\
&= (\epsilon_{j_1} + \epsilon_{j_2} + \epsilon_{j_3})\delta_{J_c',J_c} + \langle j_1 j_2; J_c'|V_{12}|j_1 j_2; J_c\rangle \, \delta_{J_c',J_c} \\
&+ \sum_{J_{13}} (-1)^{J_c'+J_c} \sqrt{(2J_c'+1)(2J_c+1)}(2J_{13}+1)\times \\
&\times \begin{Bmatrix} j_1 & j_2 & J_c' \\ J & j_3 & J_{13} \end{Bmatrix} \begin{Bmatrix} j_1 & j_2 & J_c \\ J & j_3 & J_{13} \end{Bmatrix} \langle j_1 j_3; J_{13}|V_{13}|j_1 j_3; J_{13}\rangle \\
&+ \sum_{J_{23}} \sqrt{(2J_c'+1)(2J_c+1)}(2J_{23}+1)\times \\
&\times \begin{Bmatrix} j_2 & j_1 & J_c' \\ J & j_3 & J_{23} \end{Bmatrix} \begin{Bmatrix} j_2 & j_1 & J_c \\ J & j_3 & J_{23} \end{Bmatrix} \langle j_2 j_3; J_{23}|V_{23}|j_2 j_3; J_{23}\rangle
\end{aligned} \tag{1}$$

where:
j_1, j_2 and j_3 are the spins of the particles and holes, J_c, J_c', J_{13} and J_{23} are possible intermediate spins and J is the spin of the level.

Diagonalization in J_c, J_c' gives the wave functions and energies of the states. The results for neutron excitations of ^{208}Pb are shown in Fig. 2b and for proton excitations in 2c. The highly mixed collective octupole state in ^{208}Pb cannot be included in these calculations. The associated levels in ^{209}Pb are better described by the particle-vibration coupling model. This will be treated in a forthcoming paper [17] together with the other particle-octupole states in neighbouring nuclei found in this experiment.

The three lowest levels of ^{209}Pb are the single neutron $2g_{9/2}$, $1i_{11/2}$ and $1j_{15/2}$ states. These neutron orbitals coupled to the yrast excitations of the ^{208}Pb core form also the higher yrast states of ^{209}Pb. The low spin neutron orbitals $\nu 4s_{1/2}$ and $\nu 3d_{5/2}$ are not important for the high spin states.

The $15/2^-$ state at 1423 keV contains about 30% of the $\nu 2g_{9/2} \otimes 3^-$ configuration. This is deduced from the missing strength in the $l = 7$ neutron transfer from ^{208}Pb [18] and the strength of its E3-decay, $B(E3, 15/2^- \rightarrow 9/2^+ gs) = 26$ W. u. [19]. The next level at 3047 keV has been assigned $(15/2)^-$ by Dünnweber et al. [5] and very likely contains most of the $\nu 2g_{9/2} \otimes 3^-$ configuration. Then the M1 decay to the lower $15/2^-$ level, proceeding with strong diagonal matrix elements, should dominate, and this 1624 keV transition is the only one observed experimentally.

We identify the 3092 keV level seen here with that at 3100(5) keV excited in ^{207}Pb(t,p) with $l = 8$. The calculations firmly predict the $17/2^-$ yrast state of the configuration $\nu 2g^2_{9/2} 3p^{-1}_{1/2}$ here. The energy of this level is lowered relative to the single particle energy by the attraction in the $(\nu 2g_{9/2} 3p^{-1}_{1/2},\ 5^-)$ excitation of ^{208}Pb for both $2g_{9/2}$ neutrons. The strong population of this level and its γ decay support firmly that it is an yrast state and the fact, that the only transfer reaction, that populates it, is ^{207}Pb(t,p) agrees with the configuration assignment.

The lowest state of the next higher spin $19/2^-$ is calculated to be at 3606 keV (Fig.2c) and belongs to the $\nu 2g_{9/2} \pi 1h_{9/2} 3s^{-1}_{1/2}$ configuration. Indeed the proton pick up reaction [3] from the $(\nu 2g_{9/2} \pi 1h_{9/2},\ 9^-)$ state in ^{210}Bi populates strongly a state at 3530(5) keV that fits our level at 3524 keV. A sizeable admixture of $\nu 2g^2_{9/2} 2f^{-1}_{5/2}$ is expected for this level as the 2^{nd} 5^- state in ^{208}Pb contains much $\nu 2g_{9/2} 2f^{-1}_{5/2}$. This is the likely reason, that the calculated energy for the pure configuration is 80 keV too high. The γ-decay of this level has to proceed through small admixtures of the wave functions. The spectrum of the ^{210m}Bi$(t,\alpha)^{209}$Pb reaction shows another strong transition establishing a level at 3657 keV [3] and no other lines in this region. Therefore this level is most likely the $17/2^-$ state of this configuration, which as a non yrast state is not likely observed in our experiment. The calculated $E(17/2^-) - E(19/2^-) = 158$ keV compares well with the measured 127(7) keV.

So far the basic assumption in the interpretation of the states, namely that yrast states are populated and can be identified with the shell model yrast states has been supported by transfer data. The 3810 keV level is interpreted as $\nu 2g_{9/2} \nu 1i_{11/2} \nu 3p^{-1}_{1/2}$ excitation with the maximum angular momentum of $(21/2^-)$. Its M1 decay to the $19/2^-$ state can only proceed via likely small admixtures of other configurations, while the allowed E2 decay to $17/2^-$ for the main configurations is slow with a partial halflife of $\sim$1ns. Therefore the comparable strength found in this experiment is acceptable, as the E2 decay might also be enhanced by admixtures. In particular an admixture of $\nu 2g^2_{9/2} \nu 2f^{-1}_{5/2}$ to the $21/2^-$ level has a strong E2 matrix element to the main component of the $17/2^-$ state.

The very strong 2419 keV line depopulates a level at 3842 keV. From the intensity we conclude that this is an yrast state. The most striking feature of these experiments is that the octupole excitations on top of the high spin particle or hole states are very prominent [17]. Therefore this state is most likely $(\nu 1j_{15/2} \otimes 3^-,\ 21/2^+)$ with a component of $(\nu 2g_{9/2} \otimes 3^- \otimes 3^-,\ 21/2^+)$ of similar magnitude as the one-phonon component in the yrast $15/2^-$ state. The weak E1 γ-branch to the $(19/2^-)$ level supports this, too.

The last level that can be assigned confidently to a calculated shell model state, namely $\nu 1j_{15/2} 2g_{9/2} 3p^{-1}_{1/2}$, is at 4329 keV and decays by 487 keV to $(21/2^+)$. For this configuration the highest spin state $25/2^+$ is appreciably higher, because the $(\nu 2g_{9/2} \otimes 3^-)$ admixture of the $\nu 1j_{15/2}$ orbital is blocked by the Pauli principle. One may also compare directly the experimental spacings $E(23/2^+) - E(17/2^-) = 1237$ keV in ^{209}Pb and $E(11^-) - E(8^+) = 1234$ keV in ^{210}Pb . In both cases one neutron changes from $\nu 2g_{9/2}$ to $\nu 1j_{15/2}$. The very close agreement of these two numbers may be understood as a consequence of the almost identical interaction of $\nu 3p^{-1}_{1/2}$ with $\nu 1j_{15/2}$ and $\nu 2g_{9/2}$. In fact the spacings $E(8^+) - E(5^-) = 1413$ keV in ^{208}Pb and $E(1j_{15/2}) - E(2g_{9/2}) = 1423$ keV in ^{209}Pb are also almost the same. A $23/2^-$ assignment of the configuration $\nu 1i_{11/2} 2g_{9/2} 2f^{-1}_{5/2}$ cannot be ruled out however, although E1 transitions do not compete usually with M1, if they are at all possible.

Assignments to the higher states are ambiguous. Too many configurations are possible and they might well be appreciably mixed as are the 8^+ and 10^+ states in ^{208}Pb. Also some important matrix elements of the $\nu\pi^{-1}$ interaction like $\nu 2g_{9/2} \pi 1h^{-1}_{11/2}$ have not yet been measured.

5 Conclusions

The level scheme of ^{209}Pb has been extended along the yrast line by γ-spectroscopy with deep inelastic reactions. The main features of the scheme are well explained by the shell model up to the $(23/2^+)$ state. The levels are simple two particle one hole states; therefore a more refined description, that includes configuration mixing, can add to our knowledge of the residual interaction in a direct way.

This work was partly supported by the Polish Scientific Committee grant no. 2P03B 150 10 and the polish German agreement on scientific cooperation, project X081.51. We are grateful to the German EUROBALL collaboration for making the HPGe-Cluster detectors available and to the CRYSTAL BALL collaboration for the CRYSTAL BALL.

References

1. M.J. Martin, Nucl. Data Sheets **63**, 723 (1991)
2. G. Igo, E.R. Flynn, B.J. Dropesky, P.D. Barnes, Phys. Rev. C **3**, 349 (1971)
3. Ole Hansen, Nelson Stein, D.G. Burke, E.R. Flynn, J.D. Sherman, J.W. Sunier, R.K. Sheline, Nucl. Phys. A **277**, 451 (1977)
4. E.R. Flynn, G. Igo, P.D. Barnes, D. Kovar, D. Bes, R. Broglia, Phys. Rev. C **3**, 2371 (1971)
5. W. Dünnweber, E.R. Cosman, E. Grosse, W.R. Hering, P. von Brentano, Nucl. Phys. A **247**, 251 (1975)
6. M.C. Kouassi, A. Hachem, C. Ardisson, G. Ardisson, Nucl. Instrum. Methods A **280**, 424 (1989)
7. R. Broda, B. Fornal, W. Królas, T. Pawlat, D. Bazzacco, S. Lunardi, C. Rossi-Alvarez, R. Menegazzo, G. de Angelis, P. Bednarczyk, J. Rico, D. De Acuna, P.J. Daly, R.H. Mayer, M. Sferrazza, H. Grawe, K.H. Maier, R. Schubart, Phys. Rev. Lett. **74**, 868 (1995)

8. M. Schramm, H. Grawe, J. Heese, H. Kluge, K.H. Maier, R. Schubart, R. Broda, J. Grebosz, W. Królas, A. Maj, J. Blomqvist, Z. Phys A **344**, 363 (1993)
9. M. Rejmund, K.H. Maier, R. Broda, M. Lach, J. Wrzesiński, J. Agramunt, J. Blomqvist, A. Gadea, J. Gerl, M. Górska, H. Grawe, M. Kaspar, I. Kozhoukharow, I. Peter, H. Schaffner, R. Schubart, Ch. Schlegel, G. Stengel, S. Wan, H.J. Wollersheim, Z. Phys. A **359**, 243 (1997)
10. T.T.C. Kuo, G.E. Brown, Nucl. Phys. **85**, 40 (1966)
11. E.K. Warburton, B.A. Brown, Phys. Rev. C **43**, 602 (1991)
12. R. Broda, J. Wrzesiński, T. Pawlat, B. Fornal, Z. Grabowski, D. Bazzacco, S. Lunardi, C. Rossi-Alvarez, G. de Angelis, A. Gadea, K.H. Maier, Proceedings of the Conference on Nuclear Structure at the Limits, Argonne, Illinois, July 1996, ANL/PHY-97/1, p. 276
13. W. Królas, PhD Thesis, Inst. of Nucl. Phys. Kraków Report No 1738/PL (1996)
14. Ch. Schlegel et al., GSI report to be published
15. J. Eberth, Proc. Conf. on Physics from Large γ- Detector Arrays, August 2-6, 1994, Berkeley, Ca., USA, vol. II, LBL-356
16. V. Metag, D. Habs, K. Helmer, V. v. Helmdt, H. W. Heyng, B. Kolb, D. Pelte,D. Schwalm, et al., Lecture Notes in Physics 178, ISBN 3-540-12001-7 Springer-Verlag Ber
17. M. Rejmund et al. to be published
18. G.J. Igo, P.D. Barnes, E.R. Flynn, and D.D. Armstrong, Phys. Rev. **177**, 1831 (1969)
19. C. Ellegaard, J. Kantele and P. Vedelsby, Phys. Lett. **25**B, 512 (1967)